

# Normal State Spectral Lineshapes of Nodal Quasiparticles in Single Layer $\text{Bi}_2\text{Te}_2\text{O}_6$ Superconductor

A. Lanzara,<sup>1,2</sup> P. V. Bogdanov,<sup>3</sup> X. J. Zhou,<sup>3</sup> N. Kaneko,<sup>4</sup> H. Eisaki,<sup>4</sup> M. Greven,<sup>3</sup> Z. Hussain,<sup>5</sup> and Z. -X. Shen<sup>3</sup>

<sup>1</sup>Department of Physics, University of California, Berkeley, California 94720, USA

<sup>2</sup>Materials Sciences Division, Lawrence Berkeley National Laboratory, Berkeley, California 94720, USA

<sup>3</sup>Department of Physics, Applied Physics and Stanford Synchrotron Radiation Laboratory, Stanford University, Stanford, California 94305, USA

<sup>4</sup>Electrotechnical Laboratory, Tsukuba, Japan

<sup>5</sup>Advanced Light Source, Lawrence Berkeley National Laboratory, Berkeley, California 94720, USA

(Dated: April 14, 2024)

A detailed study of the normal state photoemission lineshapes and quasiparticle dispersion for the single layer  $\text{Bi}_2\text{Te}_2\text{O}_6$  ( $\text{Bi}_2\text{Te}_2\text{O}_6$ ) superconductor is presented. We report the first experimental evidence of a double peak structure and a dip of spectral intensity in the energy distribution curves (EDCs) along the nodal direction. The double peak structure is well identified in the normal state, up to ten times the critical temperature. As a result of the same self-energy effect, a strong mass renormalization of the quasiparticle dispersion, i.e. kink, and an increase of the quasiparticle lifetime in the normal state are also observed. Our results provide unambiguous evidence on the existence of bosonic excitation in the normal state, and support a picture where nodal quasiparticles are strongly coupled to the lattice.

PACS numbers: 74.25.Jb, 74.72.-h, 79.60.-i, 71.38.-k

As a measure of the imaginary part of the single particle Green's function, photoelectron spectroscopy provides insights on the scattering processes that play a key role for the physical properties of a material. In a metallic system for example, the coupling of quasiparticles to phonons causes the photoemission line shape to evolve from a single Lorentzian-like peak, as for a Fermi liquid picture, to double or multiple peak structures [2] with a dip of spectral intensity, which correspond to the phonon energy. The coupling to phonon, or more in general to any bosonic excitation, is also reflected in a renormalization of the quasiparticle dispersion, and in an increase of the quasiparticle lifetime below the phonon energy [3]. In the framework of quasiparticles coupled to a bosonic excitation these behaviors are the result of the same self-energy effect,  $(k, \omega)$ , and occur at a similar energy scale [4].

This textbook behavior has been recently measured by angle resolved photoemission spectroscopy (ARPES) in several systems characterized by a strong electron-phonon interaction, such as Be [5], Mo [6], W [7] and  $\text{C}_{60}$  [8]. Similar behavior has also been observed in several families of p-type cuprates along the nodal direction,  $(0, 0)$  to  $(\pi, \pi)$  [9, 10, 11, 12, 13, 14, 15, 16]. While in the case of simple metals the interpretation is straightforward and phonons are easily identified as the relevant energy scale, the interpretation is far more complex in the case of strongly correlated systems as cuprate superconductors. Although the experimental data between different groups are in agreement, and are in favor of a scenario of quasiparticles coupled to bosonic modes, the nature of such excitations is still highly controversial and has been matter of intense study over the last few years.

The two proposed scenarios see quasiparticles coupled to phonons [10, 11] vs quasiparticles coupled to an electronic mode [12, 13, 14, 15, 16]. On the basis of energy scale it has been argued that, the highest energy phonon coupled to quasiparticle is the in plane halfbreathing oxygen phonons [17, 18], while the relevant electronic mode is the  $(\pi, \pi)$  resonance mode, observed by neutron scattering [19, 20]. The major difference between these two proposed scenario lies on their normal state behavior. In the case of phonons a well-defined energy scale in the normal and superconducting state is needed, while, in the case of resonance mode scenario, no energy scale is defined in the normal state, where the quasiparticle behave as Marginal Fermi liquid [21]. It has been argued that, the Marginal Fermi liquid scenario can account for the following normal state behaviors observed in  $\text{Bi}_2\text{Te}_2\text{O}_6$ : curvature in the dispersion [12] that is related to the linear energy dependence of the scattering rate [22], and the presence of an additional structure in the EDCs only in the superconducting state [12]. However there are two issues that are subjects of continuous debate. First, the marginal Fermi liquid picture itself does not define a microscopic origin so a combined electronic and phononic contribution could give rise to a behavior mimicking the Marginal Fermi liquid phenomenology. Second, and more substantively, the nodal kink is found to exist over the entire doping range [10] with similar energy scale, while the marginal Fermi liquid behavior is observed only near optimal doping. Further, the kink in the dispersion is very sharp in underdoped samples and not possible to be fitted by a smooth band as in the case of Marginal Fermi liquid.

An investigation of the normal state energy distribu-

tion curve (EDC) can provide a definitive answer to this issue. In the Marginal Fermi liquid scenario, the EDC curve is a single Lorentzian peak, where the peak width, proportional to the imaginary part of the electron self-energy, depends linearly on the frequency. This condition is dictated by the absence of any energy scale other than the high frequency cutoff in the Marginal Fermi liquid picture. In a phonon type scenario, on the other hand, the phonon energy scale will show up in the EDC spectral function, which is now characterized by a double peak structure, the so-called peak-dip-hump structure [2]. This expected contrast thus provides an acid test for the two cases. This test can be performed in the single layer B i2201 system, as we can have access to the normal state behavior without suffering from thermal effects. In addition the single layer B i2201 spectra do not suffer from bilayer splitting effect, which might make the picture more complex in the case of the double layer B i2212. Recently in fact, an alternative explanation to the nodal double peak structure observed in B i2212 [10] has been proposed [27], where the two peaks have been associated with the 0.2ps-0.2ps bands of two adjacent CuO layers [27], i.e. bilayer splitting, rather than as a signature of electrons coupled to a collective mode [2]. The existence of bilayer splitting does not rule out coupling to collective mode, something made very clear by the data from the antinode. The presence of bilayer splitting does make the data analysis more complex.

Here we report a detailed ARPES study of the normal state quasiparticles in single layer underdoped B i2201 ( $T_c = 10$  K). Our results provide the first evidence of a double peak structure in the EDCs along the nodal direction,  $(0,0)$  to  $(\pi, \pi)$ . The double peaks structure persists well above the critical temperature, up to ten times  $T_c$ . A kink in the dispersion and an increase of the quasiparticle lifetime at the dip energy are also observed. These results provide unambiguous evidence of quasiparticles coupled to bosonic excitations in the normal state, and put a strong constraint on the fundamental scattering process of cuprates, supporting a picture where phonons are strongly involved.

Angle resolved photoemission data have been recorded at beam-line 10.0.1.1 of the Advanced Light Source in Berkeley, in a similar set-up as reported previously [24]. The underdoped (UD)  $B i_{2-x}Sr_xLaCuO_{6+}$  ( $x = 0.75$ ,  $T_c = 10$  K) was grown using the coating-zone method. The data were collected utilizing 33eV photon energy. The momentum resolution was 0.14 degrees and the energy resolution 14meV. The single crystalline samples were cleaved in situ at low temperature and the samples were oriented so that the analyzer scan spans along the  $(0,0)$  to  $(\pi, \pi)$  diagonal direction. We have performed a mapping at low temperature (20 K) and a temperature dependent study along the nodal,  $(0,0)$  to  $(\pi, \pi)$ , direction. The temperature dependence was studied through a thermal cycle in order to monitor the sample quality

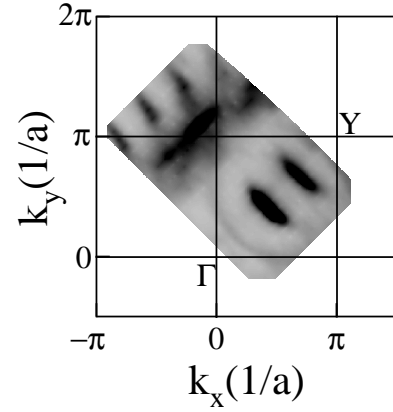


FIG. 1: Map of the ARPES intensity in the momentum space at the Fermi energy for underdoped B i2201 superconductors. The map is taken at 25K. In the maps, black corresponds to the maximum intensity and white to zero intensity.

during the experiment and the reproducibility of the observed behavior. The vacuum during the measurement was better than  $4 \times 10^{-11}$  Torr. In this paper we use the notation low and high energy to indicate energy range of  $(0, -60$ meV) and energy range of  $(-60$  to  $-300$ meV) respectively.

In figure 1, we show the map of the spectral intensity at the Fermi energy ( $E_F$ ) in the normal state, up to the second Brillouin zone (BZ). Highest intensity points in the spectral intensity map at the Fermi energy (black color) give the Fermi surface. As previously reported, the spectral weight primarily concentrates around the nodes along the  $(0,0)$  to  $(\pi, \pi)$  direction of the superconducting gap function [25, 26]. The crossing between the superstructure bands and their replica enhances the spectral weight at  $(\pi, 0)$ . The contribution coming from them and the superstructure replica are clearly seen and can be well separated in a momentum window close to the nodal direction. This global mapping allows us to locate the momentum precisely.

In figure 2, we show high-resolution energy distribution curve (EDCs), ARPES curves as a function of energy, along the nodal direction at several temperatures, up to more than ten times  $T_c$ . All the data reported here are in the normal state for  $T_c < T < T^*$ , where  $T^*$  is the pseudogap temperature. The EDCs stack shows two main features: sharp slow-dispersing low binding energy peak, crossing the Fermi energy  $E_F$ , defined to be zero throughout this paper, and, broad fast-dispersing high binding energy peak (hump). The two peaks coexist in a small momentum interval and are separated by a dip of spectral intensity at 60meV (dashed lines in the figure). Similar lineshapes have been reported in the case of Be [5] and for double layer B i2212 in the superconducting state [10]. Finally, as the temperature is raised (from 20K to 200K) the two peaks evolve in a single broad feature and the dip between them is hardly distinguishable. This is

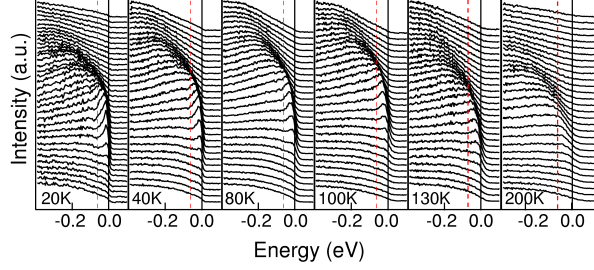


FIG. 2: Energy Distribution curves (EDC) in the normal state at several temperatures (from 20K to 200K) for the underdoped Bi2201 superconductors. All the data here shown are in the normal state. A dip in the EDCs can be clearly observed almost for all the temperatures. The dip position (dotted line) is  $\sim 60$  meV and is roughly temperature independent.

simply a thermal effect as explained before and it is observed in Bi2201 [5]. In addition, the data shown here, where a double structure can be distinguished despite the absence of bilayer splitting, clearly rule out the interpretation proposed to explain the Bi2212 double peak structure in terms of bilayer splitting [27]. Our data support therefore the following arguments: 1) Presence of a double peak structure for nodal quasiparticles; 2) Persistence of the double peak structure well above the critical temperature, suggesting that bosons with well defined frequency are coupled to quasiparticles in the normal state; 3) Temperature is the main cause of the broadening observed in the EDCs at high temperature.

In figure 3a, we show the nodal quasiparticle dispersion vs binding energy for several temperatures, same as shown in figure 2. The dispersions are extracted by fitting the momentum distribution curves (MDC), cut at fixed energy, with Lorentzian like functions. A sharp break in the dispersion, kink, is observed (see horizontal arrows in the figure), in agreement with previous results [10, 14]. Consistently with the temperature dependence of the ARPES spectra in figure 2, the kink in the dispersion is well defined up to very high temperatures. At temperatures high enough ( $\sim 130$  K) however, the kink structure becomes smoother. A similar smoothing, in the case of Bi2212, has been erroneously argued as evidence of no energy scale [12]. The data presented here in fact, clearly show that the smoothing of the kink is simply an effect of temperature broadening.

In panel b, we report the MDC width at half maximum (FWHM) vs binding energy for same temperatures as in panel a. Each curve is shifted by a constant offset (see caption). Within the sudden approximation, the MDC width is proportional to the imaginary part of the electron self-energy,  $\text{Im}(\Sigma(k, \omega))$  [4]. The FWHM consists of two components: i) a step like sudden increase near  $\sim 60$  meV, as predicted in the case of quasiparticles coupled to a sharp bosonic excitation; ii) a  $\omega^{-2}$  dependence that persists up to very high energy. The step like

structure in the FW HM is defined for all temperatures. In the hypothesis of independent scattering mechanism, valid in weak coupling regime [5, 6], the step like increase at low energy in our data can be interpreted as due to coupling to bosons. Therefore, the presence of a step like structure in the normal state is a clear evidence that similar coupling persists up to very high temperatures. This observation is also consistent with the temperature dependence of the kink in the dispersion (fig. 3a) and the temperature dependence of the double peaks structure in the ARPES spectra (fig. 2). Similar behavior of the FW HM in the normal state has been reported for the  $\text{La}_{2-x}\text{Sr}_x\text{CuO}_4$  (LSCO) compound at  $x=0.03$  doping [11]. Finally, the data here presented, clearly support a picture where coupling to the same bosonic modes is present in the normal state. In panel c we show the real part of the electron self-energy,  $\text{Re}(\Sigma(k, \omega))$ , vs binding energy in the same temperature range as in previous panels. The  $\text{Re}(\Sigma(k, \omega))$  is defined as the difference between the measured (dressed) quasiparticle dispersion, and the bare dispersion,  $\epsilon(k)$  [23]. Here we approximate the bare dispersion by a straight line connecting  $k_F$  and the dispersion at high energy 300 meV, see dotted lines in panel a), following a previous convention [12]. The value of the  $\text{Re}(\Sigma(k, \omega))$  is of course strongly dependent from our choice

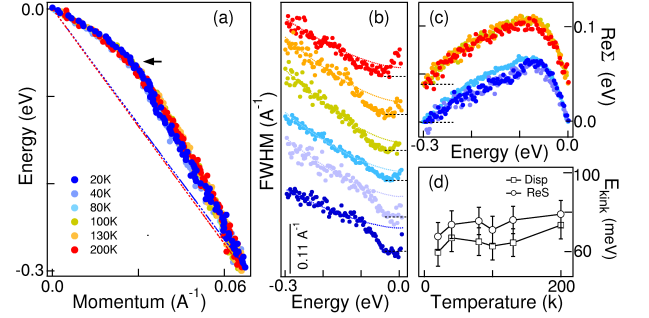


FIG. 3: a) Quasiparticle dispersions, extracted by fitting the momentum distribution curves, along the nodal direction. The dispersions are shown for same temperature range as in fig. 2. The bare quasiparticle dispersion  $\epsilon(k)$  is shown by dotted lines. Details of how to determine  $\epsilon(k)$  are given in the text. b) Width of the momentum distribution curves (FWHM) vs quasiparticle energy in the nodal direction, for underdoped Bi2201. The FWHM at each temperature are shifted by a constant offset (0.08  $\text{\AA}^{-1}$ ). A step like function is observed for all measured temperatures, however it becomes smoother as the temperature increases. The drop of the MDC width corresponds to the energy kink position. c)  $\text{Re}(\Sigma(k, \omega))$  vs binding energy determined from the difference between the measured quasiparticle dispersion and the bare dispersion (dashed line in panel a). The  $\text{Re}(\Sigma(k, \omega))$  at high temperature are shifted by a constant offset (40 meV) from the low temperature data. d) Kink energy position vs temperature as extracted by two different methods: 1) maximum position of the  $\text{Re}(\Sigma(k, \omega))$  (circles); 2) straight lines of the low and high energy quasiparticle dispersions (squares).

of  $\text{Re}(\epsilon(\mathbf{k}))$ , however this type of analysis holds for a qualitative comparison between different temperatures, since the bare dispersion should be temperature independent. The maximum position of the  $\text{Re}(\epsilon(\mathbf{k}))$  is therefore another way to identify and measure the kink position in the dispersion. At low temperatures a well-defined peak in the  $\text{Re}(\epsilon(\mathbf{k}))$  is observed.

The peak broadens as the temperature increases as a result of thermal broadening, as discussed in panels a and b. The broadening of the  $\text{Re}(\epsilon(\mathbf{k}))$  can also be predicted within an Eliashberg type electron-boson model, see ref. [23]. It is important to point out that, in the case of Bi2212, the broadening of the  $\text{Re}(\epsilon(\mathbf{k}))$  and the disappearance of the sharp peak at low energy, have been considered compelling evidence against a electron-boson interacting picture, where the broad hump in the  $\text{Re}(\epsilon(\mathbf{k}))$  is now purely dominated by electron-electron interaction [12, 28]. The data here shown, where a sharp peak in the  $\text{Re}(\epsilon(\mathbf{k}))$  is observed well above  $T_c$  suggest that temperature effect might be the cause of the broadening observed in the Bi2212 case, where  $T_c$  is higher [12, 28].

In panel d we report the energy position of the nodal kink as a function of temperature. The kink position is extracted using two correlated methods: 1) the maximum position of the  $\text{Re}(\epsilon(\mathbf{k}))$  (circles) [23]; 2) the energy intersection between the straight line fit for the low and high energy part of the dispersion [10] (squares). The data show a slight temperature dependent increase of the kink position, as explained in simple electron-boson picture [23]. The large error bars at high temperatures are due to the broader peaks with respect to the low temperature data.

In conclusion, we have shown a detailed study of the photoemission spectra in the underdoped single layer Bi2201 superconductor. We have provided the first evidence of a double peak structure in the nodal ARPES spectra up to ten times the critical temperature. The dip of the spectral weight corresponds to the same energy scale where the quasiparticle dispersion shows a kink, or similarly where  $\text{Re}(\epsilon(\mathbf{k}))$  shows a peak, and where the  $\text{Im}(\epsilon(\mathbf{k}))$  shows a step like change. All the results here presented clearly support a scenario of quasiparticles coupled to bosonic excitations with well-defined energy in the normal state. Given the absence of a resonance mode in the single layer Bi2201 and the temperature dependence behavior shown here, we conclude that the bosonic excitations are associated with coupling with oxygen related

optical phonons.

This work was supported by the Department of Energy's Office of Basic Energy Science, Division of Materials Sciences and Engineering of the U.S. Department of Energy, under Contract No. DE-AC03-76SF00098 and by the National Science Foundation through Grant DMR-0349361. SSRL work is supported by DOE contract DE-AC03-76SF00515. Stanford work is also supported by NSF DMR-0304981.

- 
- [1] P. V. Bogdanov, Phys. Rev. Lett. 85, 2581 (2000)
  - [2] D. J. Scalapino in Superconductivity (ed. Parks, R. D.) p. 449
  - [3] F. Marsiglio Phys. Rev. B 47, 5419 (1993)
  - [4] L. Hedin and S. Lundqvist in Solid State Physics, edited by Seitz, F., Turnbull, D. & Ehrenreich, H., Academic Press (1969).
  - [5] M. Hengsberger et al., Phys. Rev. Lett. 83, 592 (1999); S. LaShell, E. Jensen, and T. Balasubramanian, Phys. Rev. B 61, 2371 (2000)
  - [6] T. Valla et al. Phys. Rev. Lett. 83, 2085 (1999)
  - [7] E. Rotenberg et al. Phys. Rev. Lett. 84, 2925 (2000)
  - [8] O. Gunnarsson et al. Phys. Rev. Lett. 74, 1875 (1995)
  - [9] P. V. Bogdanov et al. Phys. Rev. Lett. 85, 2581 (2000)
  - [10] A. Lanzara et al. Nature 412, 510-514 (2001)
  - [11] X. J. Zhou et al. Nature 423, 398 (2003)
  - [12] P. D. Johnson et al. Phys. Rev. Lett. 87, 177007 (2001)
  - [13] A. Kaminski et al. Phys. Rev. Lett. 86, 1070 (2001)
  - [14] T. Sato et al. Phys. Rev. Lett. 91, 157003 (2003)
  - [15] A. D. Gromko et al. cond-mat/0202329 (2003)
  - [16] T. K. Kim et al. cond-mat/0303422 (2003)
  - [17] R. J. M. O'Connell et al. Phys. Rev. Lett. 82, 628 (1999)
  - [18] L. Pintschovius et al. Phys. Rev. B 60, 15039 (1999)
  - [19] H. F. Fong et al. Phys. Rev. B 54, 6708 (1996)
  - [20] H. He et al. cond-mat/0002013 (2000)
  - [21] C. M. Varma et al., Phys. Rev. Lett. 63, 1996 (1989)
  - [22] A. Kaminski et al., Phys. Rev. Lett. 84, 1788 (2000)
  - [23] S. Verga et al. cond-mat/0207145 (2003); to be published in Phys. Rev. B.
  - [24] P. V. Bogdanov et al. Phys. Rev. Lett. 89, 167002 (2002)
  - [25] D. S. Marshall et al. Phys. Rev. Lett. 76, 4841-4844 (1996)
  - [26] Norman, M. R. et al. Nature 392, 157 (1998)
  - [27] A. A. Kordyuk et al. cond-mat/0311137 (2003)
  - [28] H. Wang et al. Nature 427, 714 (2004)
  - [29] G. H. Gweon et al. J. Phys. and Chem. Solids 65, 1397 (2004)
  - [30] T. Cuk et al. Phys. Rev. Lett. 93, 117003 (2004)
  - [31] G. H. Gweon et al. Nature 430, 187 (2004)